RESILIENT INFRASTRUCTURE
June 1–4, 2016
RESILIENT INFRASTRUCTURE LONDON 2016

WIND TUNNEL TESTING OF RESIDENTIAL NEIGHBOURHOOD MODEL TO ANALYZE ROOF FAILURES IN HIGH WINDS

Eric R. Lalonde
Boundary Layer Wind Tunnel Laboratory, University of Western Ontario, Canada

Gregory A. Kopp
Boundary Layer Wind Tunnel Laboratory, University of Western Ontario, Canada

ABSTRACT

The EF-Scale estimates tornado wind speeds by the damage left in their wake, including the damage done to residential houses. The scale was developed based on an expert elicitation process, and so empirical testing is useful in determining its accuracy. Wind tunnel testing is often used to test low-rise buildings but building code configurations tend to be single, isolated houses, even though residential houses are much more common in suburban environments with many neighbouring buildings. The objective of this testing was to assess the roof-failure wind speeds for residential buildings in typical neighbourhood patterns and compare them to rural residence failure speeds and the EF-Scale. To this end, a 1:50 scale model of a suburban neighbourhood with 32 houses was built and tested in a wind tunnel. The effects of several variables such as wind direction and presence of dominant openings were also included in the study. After testing, it was concluded that neighbouring houses provided shielding and increased failure wind speeds in the range of 5 – 10%. Interestingly, when the shielding effects are considered, the range of failure wind speeds matches the range set out by the EF-Scale. Further work will analyze these points in greater detail.

Keywords: Low-rise buildings; Wind loads; Tornadoes; Wood-Frame Houses; EF-Scale.

1. INTRODUCTION

The destructive capabilities of tornadoes are intense, responsible for huge costs and the loss of life every year. In the United States, tornadoes cause about $10B dollars in damages every year (Simmons et al. 2015), two thirds of which occur to residential structures. For wood-frame residential houses, failure of the roofs, be it from sheathing panel loss or global roof failure, can allow water ingress and greatly increase the amount of damage (Sparks et al. 1994). In addition to this, windborne debris from these failures can strike other structures, further increasing the amount of damage (Minor 1994).

The intensities of these tornadoes are defined in Canada using the Enhanced Fujita (EF) Scale. Since sensitive anemometry equipment is easily damaged in tornadoes, the EF-Scale uses observations of Degrees of Damage (DOD) to various Damage Indicators (DI) in the tornado path to estimate its wind speed after the fact. For example, a residential house losing its roof would be DI-2, DOD-6 and has an expected failure wind speed of 195 km/h (Environment Canada 2013). Table 1 shows an excerpt of DOD-6 for one- and two-family residences in Canada.

Table 1: Excerpt of EF-Scale for one- or two- family residences

Degree of Damage	Damage Description	Expected Value (km/h)	Lower Bound Value (km/h)	Upper Bound Value (km/h)
6	Large sections of roof structure removed (more than 50%); most walls remain standing	195	165	230

To assess how residential buildings will react to tornadoes, wind tunnel testing can be used. Most wind tunnel testing for code-based design of buildings are performed on single, isolated models within the wind tunnel, which typically simulates the open terrain, rather than the more common suburban and urban terrain. However, as of 2011 only 14% of people in Ontario lived in rural areas (Statistics Canada 2011). To allow for analysis of suburban and urban residential buildings, the boundary layer of the tunnel can be set to model suburban terrain, but this is an approximation. To have a near exact simulation, multiple house models set up in the wind tunnel simultaneously are required. In other words, full neighbourhoods also need to be replicated.

Neighbourhood modelling of residential housing has been performed in previous tests, such as (Holmes et al. 1979, Holmes 1994, Gavanski et al. 2013). However, this type of testing is relatively rare and often concludes that while surrounding buildings provide both shielding from the wind and gust enhancement from the increased turbulence, the net effects are minimal.

The objective of the current testing was to examine the effects of a fairly expansive neighbourhood using failure models to see if an increased scale would lead to different results. The testing performed used a 1:50 scale neighbourhood of up to 32 houses to test them for global roof failures in a wind tunnel at varying directions of tornado level wind speeds. Figure 1 shows an image of this testing and of a model house experiencing global roof failure. In addition to this, many tests were run on a lone house model at different orientations, with and without wall openings for differing levels of internal pressure. The goal of these tests was to determine the relationship between rural and suburban houses in terms of roof failure wind speed, the effect of orientation and wall openings on these failures, and the accuracy of the EF Scale in estimating the failure speeds of a global roof failure of a residential wood-frame house.

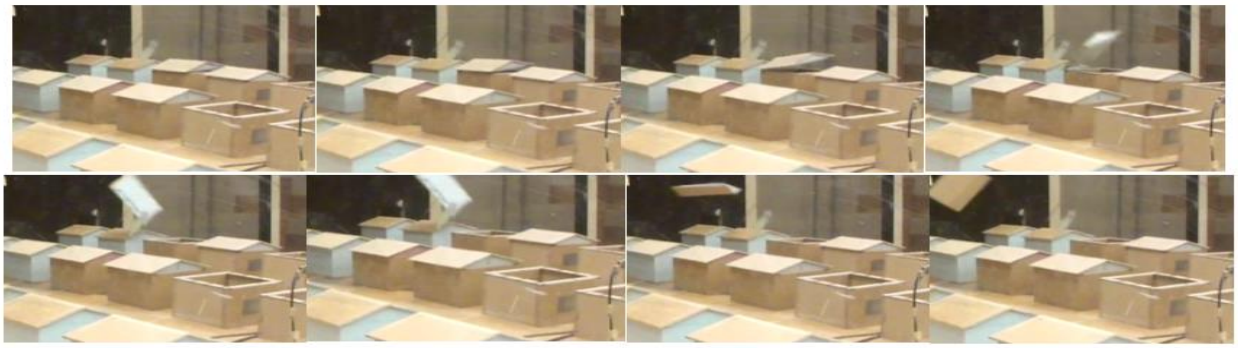

Figure 1: Global roof failure at 15 fps. The sequence is from left to right, starting in the upper row.

2. EXPERIMENTAL SETUP

2.1 House Models

Testing was performed using forty 1:50 scale-model 2-storey, 4:12-sloped, gable-roofed residential houses. Of the forty, eight of the models were “failure” models that had a roof (with a scaled mass and hold down force) that was able to experience global roof failure in the wind tunnel. This was achieved by using balsa and foam to build the roofs with magnets to simulate the hold down force of the roof-to-wall connections. These models also had openings on two sides of the house: the shorter “Front” face and the longer “Side” face. These openings represented over 2% of the given wall area, which is enough to be considered a “dominant opening” that will substantially change the internal pressure of the house (Kopp et al. 2008). These openings were covered with tape for tests with a sealed internal environment. The eight failure models were labelled A-H for testing. Figure 2 shows the dimensions of these models, and Figure 3 shows two failure models on the right.

In addition to the failure houses, there were 32 “dummy houses” which had fixed roofs that couldn’t fail. They were placed on the edge of the neighbourhood to simulate the presence of neighbouring houses for the failure models in the center. Figure 3 shows a dummy model on the left side of the failure models.

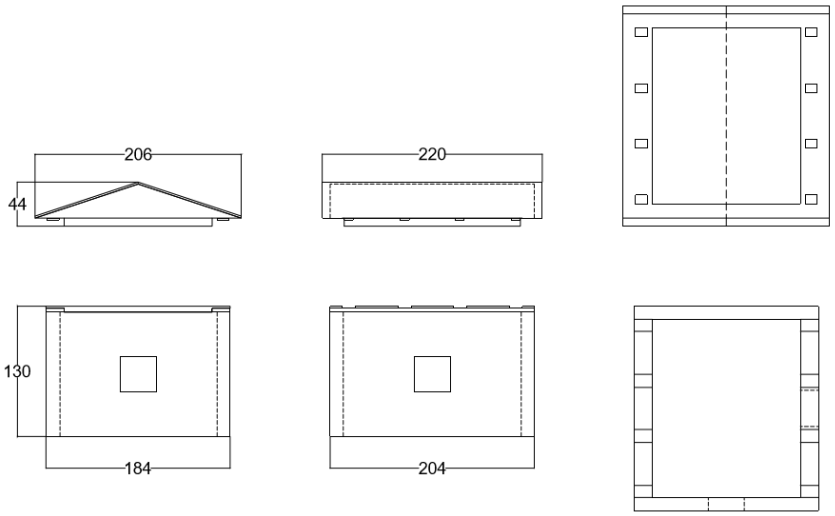

Figure 2: Failure house dimensions

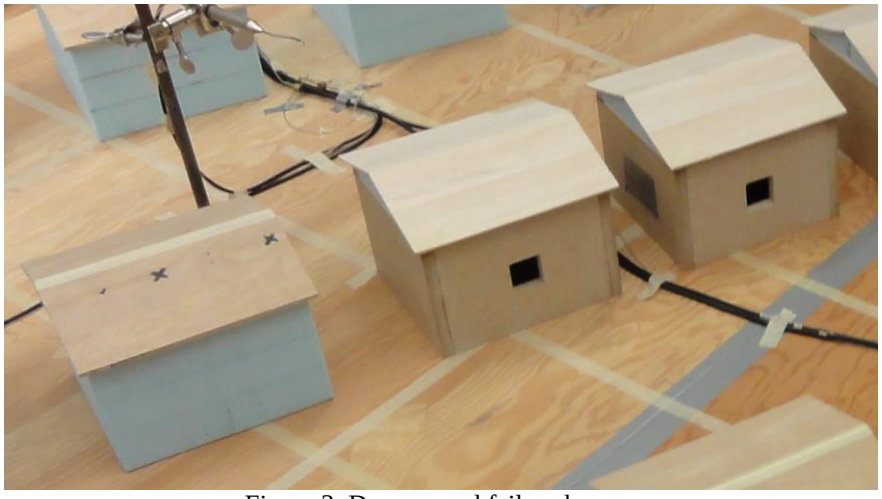

Figure 3: Dummy and failure houses

2.2 Scaling and Calibration

A scale of 1:50 for the neighbourhood was chosen because it allowed a large number of models to fit inside the wind tunnel, and also because a scale of 1:50 has been used in previous wind tunnel studies of residential houses, such as Gavanski et al. (2013). The models were designed using Froude scaling, a complete list of which can be seen in Table 2.

The model mass of the house roofs was calculated using the weight value from (Kezele 1989) and the mass scaling factor and was found to be 53.7g. This assumes a truss spacing of 0.6m, which was given by Morrison et al. (2014) as the most common wood-frame truss spacing. This spacing allowed for 18 trusses in the full scale equivalent of the failure model, the hold-down force of which was modelled using eight magnets. Toe-nails are the most common roof-to-wall connection in Ontario, thus the model hold-down force was calculated from Morrison's analysis of these connections, which found the mean failure capacity of toe-nails to be 2.8kN per connection, which, calculated using the mass scaling factor, is modelled as 82.2g. This hold-down mass was calibrated using pulleys and a hanging mass.

Table 2: Model scaling factors

Scale	Relationship	Scaling Factor
Density	$\lambda_\rho=\rho_m/\rho_p$	1
Length	$\lambda_L=L_m/L_p$	1/50
Velocity	$\lambda_U=U_m/U_p=\sqrt{\lambda_L}$	1/7.07
Mass	$\lambda_m=m_m/m_p=\lambda_\rho * \lambda_L^3$	1/125000
Time	$\lambda_L=t_m/t_p=\lambda_L/\lambda_U$	1/7.07

2.3 Neighbourhood Setup

This testing took place in Boundary Layer Wind Tunnel 1 at Western University. The model neighbourhood was placed on an 8'x8' platform. Figure 4 shows the placement of the models at different testing orientations, with the wind blowing from the north. The points of rotation for the rows of houses are the northwest corner of House E and the northeast corner of House B, which is why the arrangement of houses changes between orientations. For the 60° testing, the column spacing was reduced to main alignment with the rotation points. During single house testing, only House E was tested at the same location it is in the below figure, but with the rest of the houses removed.

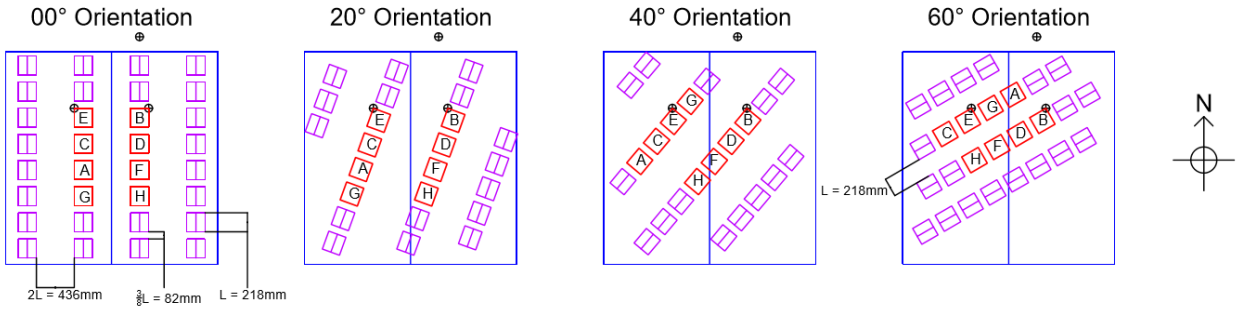

Figure 4: Model placements for different neighbourhoods

2.4 Wind Tunnel Setup and Instrument Location

The wind velocity during testing was measured by three Cobra probes, which record the wind speed and direction. Probe 289 and 290 were placed above Houses E and B, respectively, at the rotation points. They were placed at a height of 26cm above the ground, which is twice the height of the corner of the roof. As a benchmark for these probes, probe 311 was placed in front of the neighbourhood platform at the mean roof height of the failure houses. The location of the tips of the three probes can be seen above in Figure 4. The probes were attached to vertical metal stands, which would add some extra turbulence to the wind flow. However, it was decided that the presence of these probes was not dissimilar to the presence of street lights in a suburban neighbourhood, thus, they should not have impacted the test results greatly. Additionally, bird netting was strung up behind the neighbourhood to catch flying roofs and prevent them from slamming into the metal screen at the back of the wind tunnel.

Roof failure was tracked during testing using a laser transducer placed inside of House E, with the laser pointed at the front edge of the roof measuring distance. When the roof failed and was ripped from the house, the laser transducer recorded a change in distance which allowed the wind data to be aligned with the roof failure of House E.

To align the roof failures of the rest of the models, a camera was set up on a tripod outside of the wind tunnel and recorded all the neighbourhood tests. From these videos, the failure time compared to House E was found down to the nearest 30^{th} of a second (limited by the frame rate of the recording), and this value was used to find the failure wind velocities for the other house models.

During the single, isolated house testing, the Cobra probes were placed in the exact same location, and the laser transducer remained inside of House E. Video recording was not necessary for these tests, though some trials were recorded to potentially analyze failure method and roof flight.

2.5 Wind Profile

The wind tunnel roughness elements were set into an open country configuration. The resulting boundary layer can be seen in Figure 5. The reference height (H) is also the location of failure wind speed of interest: the mean roof height at 15.5cm above the ground. Since probes 289 and 290 are located at 26cm off the ground, at z/H = 26/15.5 = 1.733, the mean roof height velocity was 1/1.10 or 90% of the velocity recorded by probes 289 and 290. When z is 20cm for the full scale 10m height used in the EF scale, z/H = 1.291 and the mean roof height velocity is 96% of the velocity at 10m.

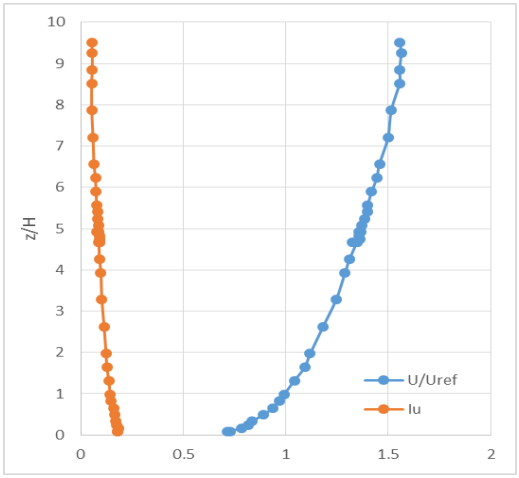

Figure 5: Wind tunnel profile and turbulence intensity for open country terrain

2.6 Test Protocols and Configurations

The fan speed of the wind tunnel was controlled via computer by raising and lowering the voltage of the fan from 0 to 10V. The single house testing was performed from an initial wind tunnel voltage intentionally below the failure wind speed, and ramped up in steps of 0.1V until failure. Each step lasted for 10 full scale minutes, as 10 minutes was considered the minimum amount of time required for statistically meaningful wind events. Using the Time Scaling Factor, the model time step duration was calculated to be 600s/7.07 = 85s. For this testing, a variety of angles and number of openings were used. The comprehensive list of tests can be found in Table 3 below.

For the neighbourhood tests, the same 85 second time step was used but each trial required many more steps. Wind tunnel voltage began at 8.6V and was increased 0.2V every step, eventually to 10V. This range was required because a variety of wind velocities were required for failure depending on the location in the neighbourhood of the failure models. In all of these tests, the side openings of the models were uncovered, while the front openings were taped close. The reason that the 00° oriented neighbourhood test is absent from Table 3 is that the wind tunnel proved too slow to cause failure in that configuration.

Table 3: Testing configurations and order

Test	Other Houses?	Wind Direction	Number of Exposed Openings	Number of Trials
S1	Single	00°	2	20
S2	Single	00°	1	10
S3	Single	00°	0	10
S4	Single	60°	1	10
S5	Single	40°	1	10
S6	Single	20°	1	10
S7	Single	20°	0	10
N1	Neighbourhood	20°	1	14
N2	Neighbourhood	40°	1	8
N3	Neighbourhood	60°	1	8

To extract the instantaneous failure velocity from the data, the maximum value from a 33ms range centered on the time of roof failure was used. This was done because the recordings of the roof failures were done at 30fps, meaning that the maximum accuracy in determining the point of failure was 1/30th of a second or 33ms. For 3s average failure velocity, a time factor scaled 0.424s average was taken, centered on the point of failure.

3. RESULTS

3.1 Single House Testing

Table 4: Single house testing summary

Test	289 Average Instantaneous Longitudinal Failure Velocity at Mean Roof Height $U_{289\text{-}I}$ (m/s)	Standard Deviation $\sigma_{289\text{-}I}$ (m/s)	Ratio of 289 Failure Velocity Over 311 Failure Velocity $U_{289\text{-}I} / U_{311\text{-}I}$	289 Average 3s Average Longitudinal Failure Velocity at Mean Roof Height $U_{289\text{-}3}$ (m/s)	Standard Deviation $\sigma_{289\text{-}3}$ (m/s)
S1	8.249	0.664	1.259	7.063	0.497
S2	6.203	0.566	1.040	5.552	0.514
S3	9.381	0.936	1.239	8.104	0.545
S4	7.587	0.968	1.180	6.785	0.521
S5	7.666	0.723	1.098	6.784	0.472
S6	8.986	1.111	1.204	7.506	0.639
S7	9.878	1.188	1.151	8.303	0.639

The above table summarizes the single house testing results. It uses the wind velocity data from probe 289 as that was the probe directly above House E, includes both instantaneous and 3s average failure speeds and their standard deviations, all reduced to 90% to lower the speed to the mean roof height. Finally, the ratios between the instantaneous velocities compared to the wind speeds at the same height in front of the testing platform were found. Most analysis was performed using the 3s average failure velocities, since they had a lower standard deviation and are the values used in the EF Scale.

By comparing tests S3, S4, S5 and S6 (each tested a single house with the front opening sealed), the effect of the orientation of the house on the failure wind speed can be analyzed. By comparing the average 3s failure velocities, Figure 5 was obtained. The graph correlates a larger orientation angle with a lower failure velocity, likely from the increased exposure of the Side Opening to the longitudinal wind, as well as from aerodynamic effects.

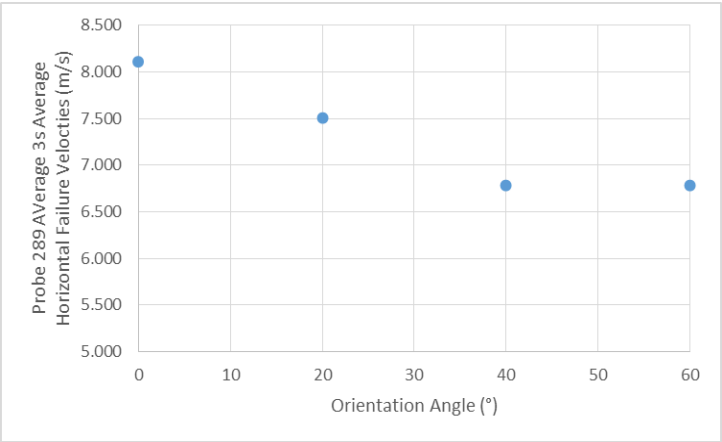

Figure 6: Orientation vs failure velocity for single opening single house tests

The effect of the dominant openings can analyzed by comparing Test S3 to Test S2 and S7 to S6. Each pair of tests feature House E at the same orientation, either sealed or with an unsealed dominant opening. Table 5 summarizes this comparison. This test wasn't performed for orientations of 40° and 60° because they failed to fail at the maximum wind speed of the wind tunnel when sealed. This shows that, while sealed, when the orientation changes from 00° to 40°, the failure velocity increases, meaning that aerodynamically the models are most vulnerable at an orientation of 00°. In terms of the dominant openings, this data shows that they reduces failure velocity by increasing internal pressure, and the magnitude of this reduction appears to increase the closer the opening is to directly facing the wind.

Table 5: Number of openings vs failure velocity for single house tests

Orientation	289 Average 3s Average Longitudinal Failure Velocity at Mean Roof Height – One Opening $U_{289\text{-}3}$ (m/s)	289 Average 3s Average Longitudinal Failure Velocity at Mean Roof Height – No Openings $U_{289\text{-}3}$ (m/s)	Ratio of No Opening Velocity Over One Opening Velocity
00°	5.552	8.104	1.460
20°	7.506	8.303	1.106

The above data only analyzed the longitudinal component of the velocity, but to properly analyze the turbulence of the neighbourhood, all the components of the velocity must be considered. As of writing, only tests S1-S3 have been analyzed in this manner, which Table 6 summarizes below. Figure 7 explains the directions and the angle directions. The data reveals that the lateral and vertical failure velocities are much smaller than the longitudinal velocities, which are to be expected. The other take away is that all failures had an upwards component which likely assisted in lifting the roof and causing failure.

Table 6: Single house multi-directional analysis summary

Test	289 Average 3s Average Longitudinal Failure Velocity at Mean Roof Height $U_{289\text{-}3}$ (m/s)	289 Average 3s Average Lateral Failure Velocity at Mean Roof Height $V_{289\text{-}3}$ (m/s)	289 Average 3s Average Vertical Failure Velocity at Mean Roof Height $W_{289\text{-}3}$ (m/s)	289 Average 3s Average Failure Velocity at Mean Roof Height $K_{289\text{-}3}$ (m/s)	Horizontal Angle of Failure Velocity (rads)	Vertical Angle of Failure Velocity (rads)	289 Failure Velocity Normalized Over 311 Failure Velocity $K_{289\text{-}3}$ / $K_{311\text{-}3}$
S1	7.075	-0.191	0.306	7.084	-0.0270	-0.0432	1.180
S2	5.552	-0.197	0.376	5.568	-0.0355	-0.0675	1.124
S3	7.996	-0.502	0.765	8.049	-0.0627	-0.0954	1.160

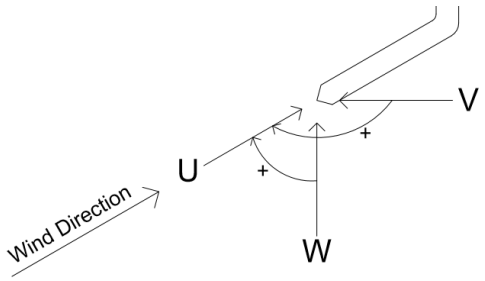

Figure 7: Angle and direction compass

3.2 Neighbourhood Testing

Table 7: 20° neighbourhood testing summary

Failure Model	Failure Percentage	Probe Used For Velocity	Average 3s Average Longitudinal Failure Velocity at Mean Roof Height U_3 (m/s)	Standard Deviation (m/s)	Full Scale 3s Average Failure Velocity at 10m U_{3F} (m/s)	Full Scale 3s Average Failure Velocity at 10m U_{3F} (km/h)	Ratio of Failure Velocity Over 311 Failure Velocity U_3 / U_{311-3}
A	46.2%	289	7.410	0.604	54.52	196.3	1.165
B	100.0%	290	7.421	0.482	54.60	196.6	1.078
C	30.8%	289	6.783	0.653	49.91	179.7	0.960
D	92.3%	290	7.259	0.686	53.42	192.3	1.161
E	100.0%	289	8.138	0.585	59.88	215.6	1.277
F	46.2%	290	6.940	0.588	51.06	183.8	1.278
G	100.0%	289	6.882	0.966	50.64	182.3	1.101
H	61.5%	290	6.399	0.603	47.09	169.5	1.098

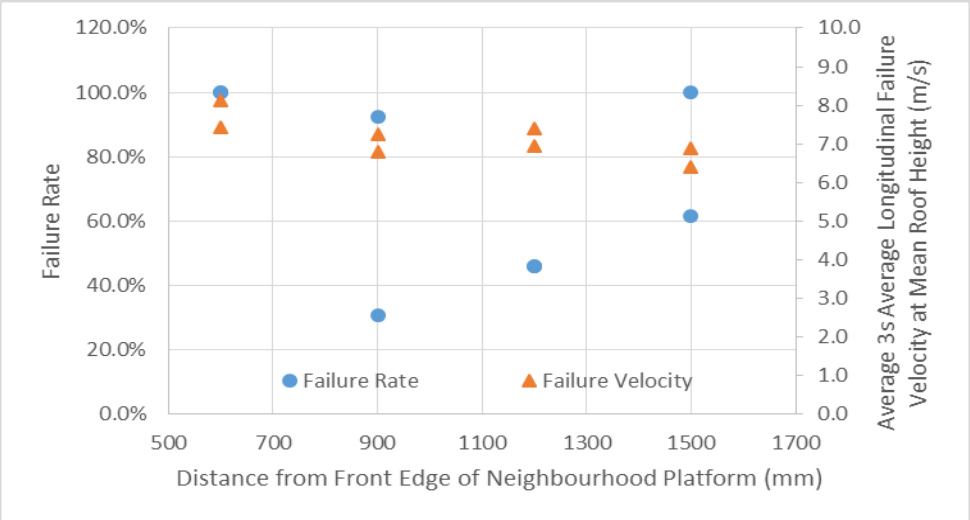

Figure 8: Failure rate and failure velocity vs location in 20° neighbourhood

As of writing, only the 20° neighbourhood test has been analyzed for longitudinal winds. Looking at Figure 8, there didn't seem to be a strong correlation between failure rate and location, thus the differences in failure rates likely stem from the slight variations in the hold-down force of the individual models. Further analysis will normalize the results against these variations to determine the true relation. The location did seem to affect the 3s average failure velocity, however. Generally, the further back the models, the lower the failure wind speed. This could have been a result of the roofs of the back models experiencing less shielding from the wind after the models in front of them failed, while the models in the front always experienced this shielding from the dummy houses. Further analysis of the failure velocities in Table 7 shows that the equivalent full scale 10m 3s average failure velocities ranged from 170-215km/h, which lies exactly within the 165-230km/h wind speed range for residential global roof failures given by the EF Scale.

Comparing the probe 311 failure velocity ratios from the single and neighbourhood tests, a similar range of values is found. The average of all the longitudinal single house tests was 1.167 and the average for the 20° neighbourhood test was 1.141, a difference of 2.2%. This suggests that the magnitude of the longitudinal component of the wind velocity is not affected severely by the presence of the neighbourhood.

Table 8 compares the failure velocities of House E in the 20° single house test to those of House E in the 20° neighbourhood test. It shows that while in the neighbourhood, House E had a greater failure velocity, suggesting that the shielding provided by the surrounding houses and increased the capacity by a small amount. If the largest measured 10m 3s average failure speed (215.6km/h) is increased by this 8.4% ratio, a value of 231km/h is obtained, which lies at the very top of the EF range for roof failures.

Table 8: Single house vs neighbourhood 20°, single opening 3s average failure velocity comparison

Single House 289 Average 3s Average Longitudinal Failure Velocity at Mean Roof Height U_{289*3} (m/s)	Neighbourhood 289 Average 3s Average Longitudinal Failure Velocity at Mean Roof Height U_{289*3} (m/s)	Ratio of Neighbourhood Failure Velocity Over Single House Failure Velocity
7.506	8.138	1.084

4. CONCLUSIONS

Through the wind tunnel analysis of the residential house models, in both single and neighbourhood configurations, at varying orientations and with differing numbers of dominant openings, the following statements could be concluded. Though, since further data analysis shall be done for these tests, there are further conclusions to be made, and the current conclusions will be refined as a result.

- The internal pressures generated by dominant openings play a large part in global roof failures. The closer one of these openings is to directly facing the longitudinal wind flow, the greater the effect of reducing failure wind speed. Of all the wind angles tested, the 00° orientation was found to be the most vulnerable, yet was found to be the most safe when a side opening was unsealed.

- When all the components of wind velocity are considered, the longitudinal wind speed is by far the largest component (which is to be expected). More notably, in all the tests analyzed thus far, there was an upwards vertical component to the velocity, which is likely helping to fail the roof.

- From the neighbourhood testing, there appears to be a correlation between the location of a failure model and the failure wind speed. The downwind models failed at lower speeds than the upwind ones, which may be due to the reduced shielding experienced when the roofs of upwind houses fail.

- Based on the 20° tests, it seems that the presence of the neighbourhood provides shielding and increases the failure wind speed of the models. The specific tests gave a required wind speed increase of 8.4% to cause failure. This increase is close to the approximately 6% increase found by Gavanski et al. (2013), who ultimately concluded that the shielding provided by neighbourhoods was ultimately minimal and extra consideration isn't required. The data obtained during this testing would suggest that they are correct.

- The 10m 3s average failure velocities (those used by the EF scale) of the 20° neighbourhood test all fell within the range given by the EF code for the global failure of the roof of a One- or Two-Family Residence. This gives more credibility to the expert opinions upon which the EF Scale is based. The fact that the testing range of 170-215km/h is closer to the bottom than the top of the 165-230km/h range given by the EF-Scale is the slight shielding cause by the neighbouring houses. When the shielding is taken into account, the maximum equivalent single house failure velocity is at the very top of the EF range. This further supports the EF Scale since the range must encompass both rural and suburban values, and the results from the testing is perfectly encompassed for this range.

ACKNOWLEDGEMENTS

This research was funded by NSERC through the USRA and Discovery Grants programs. E. R. Lalonde gratefully acknowledges the aid of Mr. Chieh-Hsun Wu in testing and data analysis, Mr. Aaron Jaffe for his part in designing and building the models, and Mr. Chris Vandelaar of University Machine Services for his guidance on model construction.

REFERENCES

Environment Canada. 2013. *Enhanced Fujita Scale (EF-Scale)*, accessed on Feb 08, 2016 from https://www.ec.gc.ca/meteo-weather/default.asp?lang=En&n=41E875DA-1

Gavanski, E., Kordi B., Kopp, G.A. and Vickery P.J 2013. Wind Loads on Roof Sheathing of Houses. *Journal of Wind Engineering and Industrial Aerodynamics*, 114, 106-121.

Holmes, J.D. 1994. Wind pressures on tropical housing. *Journal of Wind Engineering and Industrial Aerodynamics*, 53 (1–2), 105–123.

Holmes, J.D. and Best, R.J. 1979. *A Wind Tunnel Study of Wind Pressures on Grouped Tropical Houses*, Wind Engineering Report 5/79, James Cook University of North Queensland, Townsville, Australia.

Kezele, D.B.A. 1989. *Global Roof Failures of Modern Buildings*, Graduation Thesis, Department of Civil and Environmental Engineering, University of Western Ontario, London, Canada.

Kopp, G.A., Oh, J.H., and Inculet, D.R. 2008. Wind-induced internal pressures in houses. *Journal of Structural Engineering*, 134(7): 1129–1138.

Minor, J.E. 1994. Windborne debris and the building envelope. *Journal of Wind Engineering and Industrial Aerodynamics*, 53 (1–2), 207–227.

Morrison, M.J., Kopp G.A., Gavanski E., Miller C. and Ashton A. 2014. Assessment of Damage to Residential Construction from the Tornadoes in Vaughn, Ontario, on 20 August 2009. *Canadian Journal of Civil Engineering*, 41, 550-558.

Simmons, K.M., Kovacs, P., and Kopp, G.A. 2015. Tornado damage mitigation: benefit/cost analysis of enhanced building codes in Oklahoma. *Weather, Climate and Society*, 7 (2), 169-178.

Sparks, P.R., Schiff, S.D., and Reinhold, T.A. 1994. Wind damage to envelopes of houses and consequent insurance losses. *Journal of Wind Engineering and Industrial Aerodynamics*, 53 (1–2), 145–155.

Statistics Canada. 2011. *Population, Urban and Rural, by Province and Territory (Ontario)*, accessed on Feb 08, 2016 from http://www.statcan.gc.ca/tables-tableaux/sum-som/l01/cst01/demo62g-eng.htm